SUPPORTING INFORMATION

Development of a Ba-CoCe Catalyst for the Efficient and Stable Decomposition of Ammonia

Natalia Morlanés,[a] Salvador Sayas,[a] Genrikh Shterk,[a] Sai P. Katikaneni,[b] Aadesh Harale,[b] Bandar Solami[b] and Jorge Gascon* [a]

[a] *KAUST Catalysis Center (KCC), King Abdullah University of Science and Technology (KAUST), Thuwal 23955-6900, Saudi Arabia*
[b] *Carbon Management R&D Division, Research and Development Center, Saudi Aramco, Dhahran, Saudi Arabia 31311*

Catalyst synthesis

Cobalt based catalyst, Ba-CoCe, were synthesized by coprecipitation method, with Ba incorporated by impregnation. Samples with different Co/Ce molar ratio in the range 50/50 to 95/5, and Ba loading in the range 0.25-1% wt. were prepared.

Cobalt and cerium carbonates were obtained by co-precipitation using Sodium carbonate as the precipitant agent. In order to obtain samples with different Co/Ce molar ratios (50/50, 70, 30, 80/20, 90/10 and 95/5), appropriate amounts of $Co(NO_3)_2.6H_2O$ (1.82 - 3.46g) and $Ce(NO_3)_3.6H_2O$ (2.71 – 0.27g), a total of 0.0125 mol of Co and Ce, were dissolved in 25 mL of distilled water. The 0.5 M solution of nitrates was warmed up to 40 °C. Then, a warm solution of 1.65 g of Na_2CO_3 (Sigma-Aldrich) dissolved in 25 ml of distilled water, was slowly added to the Co/Ce solution, and kept under vigorous stirring for 1 hour at room temperature. The obtained precipitated of cobalt and cerium carbonates was filtered under reduced pressure and washed with cold distilled water several times until pH = 7. The resulting purple materials were dried at 100 °C overnight and calcined for 3h at 550 °C. The resulting black powder of cobalt oxide or Co_3O_4/CeO_2 composite oxides were impregnated using an aqueous solution of barium nitrate (Sigma-Aldrich) to achieve a nominal concentration of 0.25-1% wt., for the best Co/Ce catalysts with molar ratio (80/20). The resulting precursor was then dried at 120 °C overnight and then subsequently calcined at 550 °C for 3h. The final step of preparation was crushing and sieving the solid materials to get the 0.3 - 0.5 μm fraction.

A Ru-based reference material was used in the present study. The Ru supported in CaO, MgO or CeO_2 catalysts, with 3% wt. Ru loading and promoted with K (10 wt%) were prepared according to previously reported procedures using the commercial CaO, MgO and CeO_2 (Sigma-Aldrich).[1-3] Briefly, Ruthenium (III) chloride rehydrated (Sigma-Aldrich) was selected as the Ru precursor, and it was incorporated on the different supports by incipient wetness impregnation using acetone, in order to achieve different Ru loadings (3 wt. %). After drying at 60°C for 3 hours, and a subsequent thermal treatment under argon at 500 °C for 3 hours, the potassium promoter was introduced by incipient wetness impregnation using KOH in ethanol, to reach the desired K loading (10 wt.%). Finally, a second thermal treatment under Ar at 500 °C during 3h was performed.

Several samples were prepared by cobalt impregnation on commercially available ceria, CeO_2 (Sigma-Aldrich), using an aqueous solution of cobalt nitrate (Sigma-Aldrich) to achieve a nominal concentration of 2-30% wt. The resulting precursor was then dried at 120 °C overnight and then subsequently calcined at 550 °C for 3h.

Catalyst characterization

Inductively Coupled Plasma−Optical Emission Spectrometry (ICP-OES) was used to analyze the composition and metal loadings of the catalysts, on a Thermo-Electron 3580 instrument. The analyses were carried out after digestion of the solid samples. Complete digestion of the powders was achieved using aqua regia in a ratio of 1 mg of catalyst: 1 mL of aqua regia for 24 h at room temperature.

Nitrogen Adsorption and desorption isotherms were recorded on a Micromeritics ASAP 2040 system at 77 K. Samples were previously evacuated at 373 K for 16 h. The Brunauer−Emmett−Teller (BET) method was used to calculate the specific surface area. The P/P_0 range for BET analysis was $0.067 < P/P_0 < 0.249$.

X-ray Diffraction (XRD) patterns were obtained using a Bruker D8 instrument in Bragg−Brentano configuration using Cu Kα radiation. The diffractograms were scanned with a step size of 0.02° in the 2θ range of 10−90°. The crystalline phase was identified by comparison with the Joint Committee on Powder Diffraction Standards (JCPDS). Samples prepared to collect the XRD patterns after the reduction treatment (Figure 2), under hydrogen (25 mL min^{-1}) at 500°C for 3h using a ramp of 5°C min^{-1}, were passivated under 1%O_2 atmosphere at room temperature for 2 h before being exposed to the air, to prevent fast reoxidations.

Temperature programmed reduction (H_2-TPR) measurements of the samples were conducted in a U-shape reactor in Altamira instruments, by heating the samples in 5% H_2/Ar (30 mL min^{-1}) at a linear heating rate of 10 °C min^{-1} to 530 °C.

H_2-TPD measurements were carried out using fully automated AutoChem 2920 (Micromeritics Instrument Co.) in a flow set supplied with high purity gases (total gas flow rate 40 ml min^{-1}) in a quartz U-tube reactor. The detailed experimental procedure was previously described.[4-7] Briefly, in the first step catalysts the samples (0.4 g) were reduced at 500 °C for 6 h in a H_2:Ar = 80:20 mixture (40 ml min^{-1}). After flushing with Ar (40 ml min^{-1}) for 45 min, and after cooling down to 150 °C, the H_2 chemisorption was carried out for 15 min under these conditions. Then, temperature was lowered to 0 °C using a ramp of 20°C min^{-1}, and H_2 sorption continued under these conditions for 10 min. Then, the sample was flushed with Ar to remove weakly adsorbed hydrogen for 30 min. Next, the catalyst was heated under Ar constant flow (40 ml min^{-1}) using a ramp of 20°C min^{-1}, and the concentration of H_2 in the outlet gas was monitored using a mass spectrometer coupled to the outlet of the chemisorption instrument. The integration of the H_2 desorption profile allows the determination of the H_2 desorbed from the metallic Co surface. The hydrogen uptake value was used to calculate the number of active sites assuming H:Co surface= 1:1 stoichiometry of adsorption,[8] and subsequently, to estimate the dispersion of cobalt and the cobalt surface area, according to the assumption about sphericity of cobalt crystallites. The number of active surface sites, cobalt dispersion (FE, mean fraction of the total atoms exposed at the surface) and the surface of cobalt active phase were calculated from the generalized equations and proposed by Borodzinski and Bonarowska.[9-10]

Dispersion: $FE(\%) = 6\ (v_m/a_m)/d$
$S_{Co}\ (m^{-2}\ g) = 60000\ f_{Co}/(\rho \times d)$
$NA\ (mol\ g^{-1}) = f_{Co} \times FE / M$
Where:
a_m (Å^2): The surface area occupied by an atom of metal on a polycrystalline surface. 11 Å^2 for Co.
v_m (Å^3): The volume occupied by an atom of metal in the bulk of metal; 5.43 Å^3 for Co.

d: mean particle size (Å)
ρ: density of the metal in g cm^{-3}
f_{Co}: Cobalt loading in the sample, mass fraction wt.
M: molar mass of the metal, 58.93 g mol^{-1} for Co.
D: dispersion (FE, mean fraction of the total atoms exposed at the surface)
S_{Co}: Specific metal surface area in m^{-2} g
NA: number of active surface sites in mol g^{-1}

Transmission electron microscopy (TEM) of the samples was performed with a Titan Themis-Z microscope from Thermo-Fisher Scientific operated at accelerating voltage of 300 kV and beam current of 0.5 mA. Dark-field imaging was performed by scanning TEM (STEM) coupled to a high-angle annular dark-field (HAADF) detector. Furthermore, a high throughput X-ray energy dispersive spectrometer (EDS) was also utilized in conjunction with DF-STEM imaging to acquire STEM-EDS spectrum-imaging datasets. During the acquisition of these data sets, at every image pixel, a corresponding EDS spectrum was also acquired to simultaneously generate the elemental maps of Co, Ce and Ba atoms. It is also pertinent to note herein that spectrum-imaging data sets were acquired in so-called frame mode, in which the electron beam was allowed to dwell at each pixel for only a few microseconds in order to keep the total frame time to 6 s or less. Both imaging and spectroscopy data sets for each sample were acquired as well as analyzed with a newly developed software package called Velox from Thermo-Fisher Scientific. The elemental maps for Co, Ce, Ba atoms were computed using the extracted intensities of their respective Kα lines after background subtraction. The generated maps were slightly post-filtered by applying a Gaussian filter (σ = 0.5). Samples prepared for TEM analysis (Figure 4, 5, S5), after the reduction treatment under hydrogen (25 mL min^{-1}) at 500°C for 3h using a ramp of 5°C min^{-1}, were passivated under 1%O_2 atmosphere at room temperature for 2 h before being exposed to the air, to prevent fast reoxidations.

NAP-XPS measurements were carried out with an EnviroESCA spectrometer (SPECS GmbH) equipped with a monochromatic AlKα x-ray source (hν = 1486.6 eV) operating at 42 W and X-Ray emission 3.00 mA. Spectra were collected at fixed analyzer pass energy 20 eV. Photoelectron peak C1s (284.8 eV for adventitious carbon and u''' Ce^{4+} 916.7 eV) was used for a binding energy correction. For NAP-XPS studies typically ~15 mg of the samples were used to form a pellet inside the hole of the sample holder and evacuated for a 2-3 hours until pressure $9 \cdot 10^{-7}$ mbar was reached in the loading chamber. For modelling the reaction conditions ~7 mbar of gases (Ar, H_2) were individually fed into analysis section of the spectrometer with flow ratio 1:1 with an overall flow 12 ml min^{-1}. Temperature was tracked with Type K thermocouples fixed on the sample holder and maintained at 500±1°C for two hours. Deconvolution of peaks according to previously reported protocols.[11-13] Co_3O_4 as a 3 peak model where FWHM, Area, and peak positions are strictly constrained to the main peak. And Co metal as one asymmetric peak with a peak shape LA (1.2,5,5) and three satellites which are fully constrained to the main peak, following reported procedure.[12]

Catalytic activity

Ammonia decomposition catalytic tests were carried out in a PID Microactivity Reference system, using a continuous fixed bed stainless steel reactor coated with alumina to avoid any activity of the reactor. Prior to the activity measurement, the catalysts (200 mg pelletized between 300 μm and 500 μm and diluted with 1g of SiC) were reduced/activated in situ with hydrogen (25 mL min^{-1}) at 500°C for 3h, using a ramp of 5°C min^{-1}. The catalytic performance was evaluated at different temperatures

in the range 250-550 °C. For the experiments at atmospheric pressure, ammonia in the gas phase (30-100 mL min^{-1}, WHSV=9000-30000 mL g_{cat}^{-1} h^{-1}) was flown, using a mass flow controller, over the catalytic bed. Reaction products (nitrogen, hydrogen and ammonia) were analyzed under isothermal conditions with an online gas chromatograph (3000A Micro-GC gas analyzer, Agilent) using helium (1 ml min^{-1}) as internal standard for quantitative analysis. The Micro-GC is equipped with two columns: a PLOTU precolumn/Molsieve column using argon as the carrier gas for nitrogen and hydrogen; and a PLOTU column with helium as a carrier gas for ammonia. Both columns are equipped with thermal conductivity detectors.

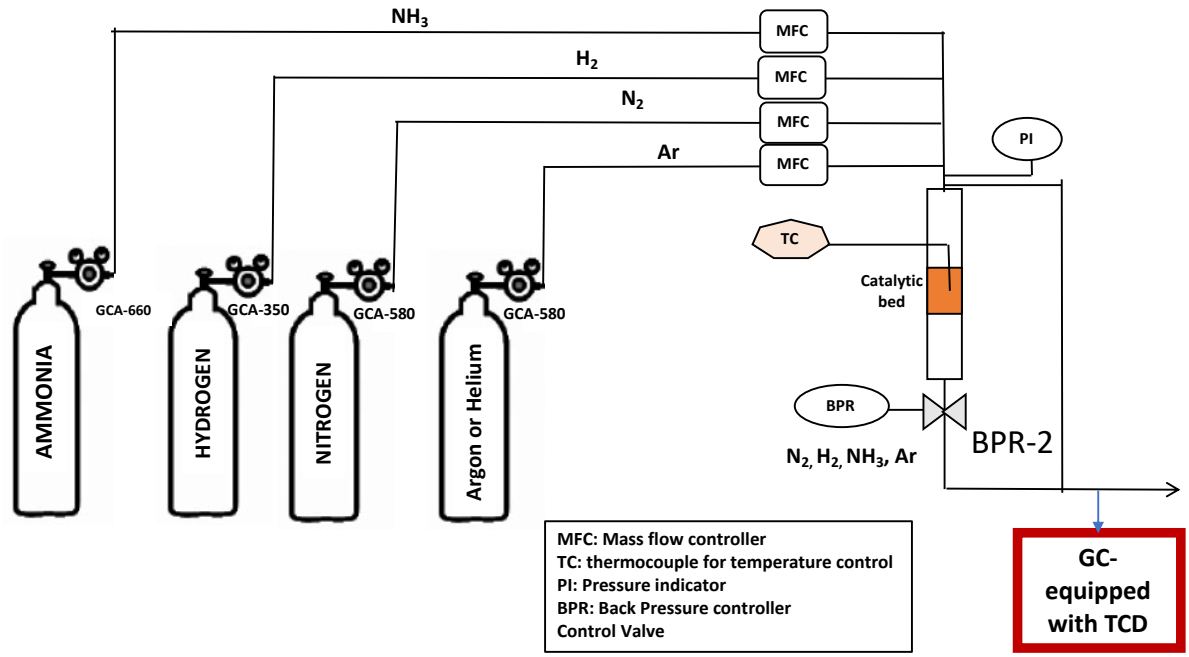

Figure S1. Experimental setup used for the study of ammonia decomposition reaction.

Kinetic studies

The kinetic analysis was performed for the samples with and without Barium, 0.5%Ba-Co/Ce (80/20) and Co/Ce (80/20), respectively. Figure 9 shows the activation energies, the reaction orders with respect to ammonia and hydrogen and the relationship between conversion and space velocity in the range WHSV=9000-30000 mL g_{cat}^{-1} h^{-1}, changing the ammonia flowrate in the range 30-100 mL min^{-1}. The reaction rates were calculated from the ammonia conversion values considering a differential reactor. Different partial pressures of both reactant and products were used in order to obtain the reaction orders for NH_3, H_2 and N_2, the results are plotted in Figure 9. The reaction conditions used are a total flow rate of 30 ml min^{-1} of mixed gas (NH_3, N_2, H_2, Ar), at atmospheric pressure and 350°C. The reaction order with respect to NH_3 was obtained by changing the flow rate in the range 5-30 ml min^{-1} and Ar balance. For the H_2 order, the NH_3 flow rate was 7.5 ml min^{-1} kept constant, and the flow rate of H_2 in the range 5-22.5 ml min^{-1} with Ar balance. For the N_2 order, the NH_3 flow rate was 22.5 ml min^{-1} (kept constant), and the flow rate of N_2 in the range 1-7.5 ml min^{-1} with Ar balance. Reaction order for nitrogen was found to be zero for both catalysts explored (not shown).

The reaction rates were calculated from the ammonia conversion values assuming a differential reactor. The activation energies were calculated from the slope of the ln(rate) vs. 1/T plots.

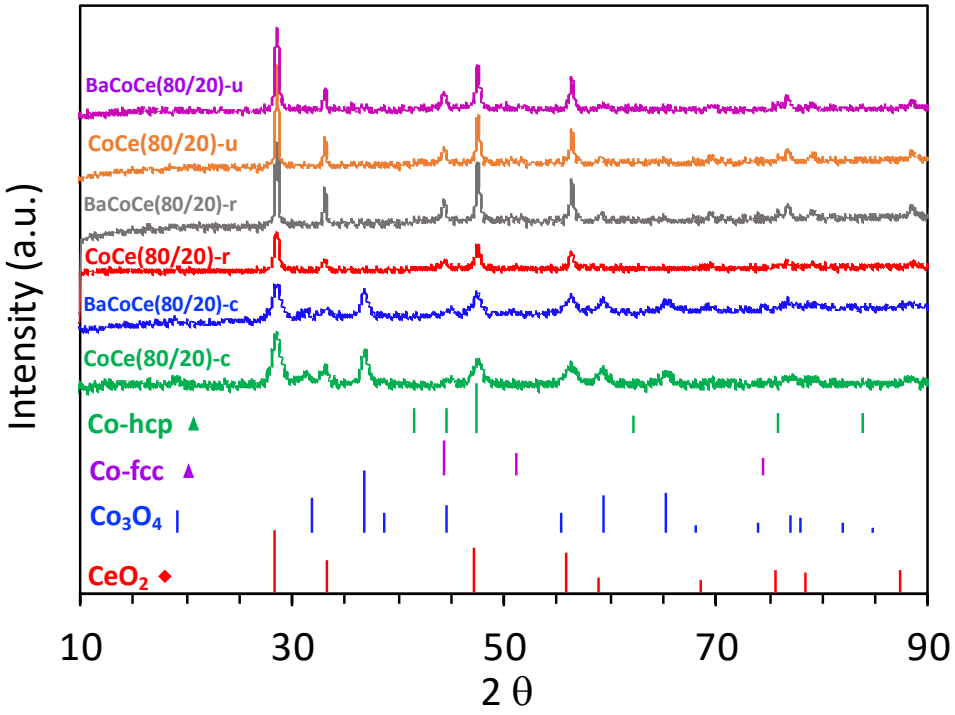

Figure S2. XRD patterns of Ba-CoCe catalysts. Suffix -c denotes after calcination at 550 °C for 3h, -r denotes after reduction under hydrogen at 500 °C for 3h and -u denotes used under ammonia decomposition reaction conditions P_{atm} and 250-550°C.

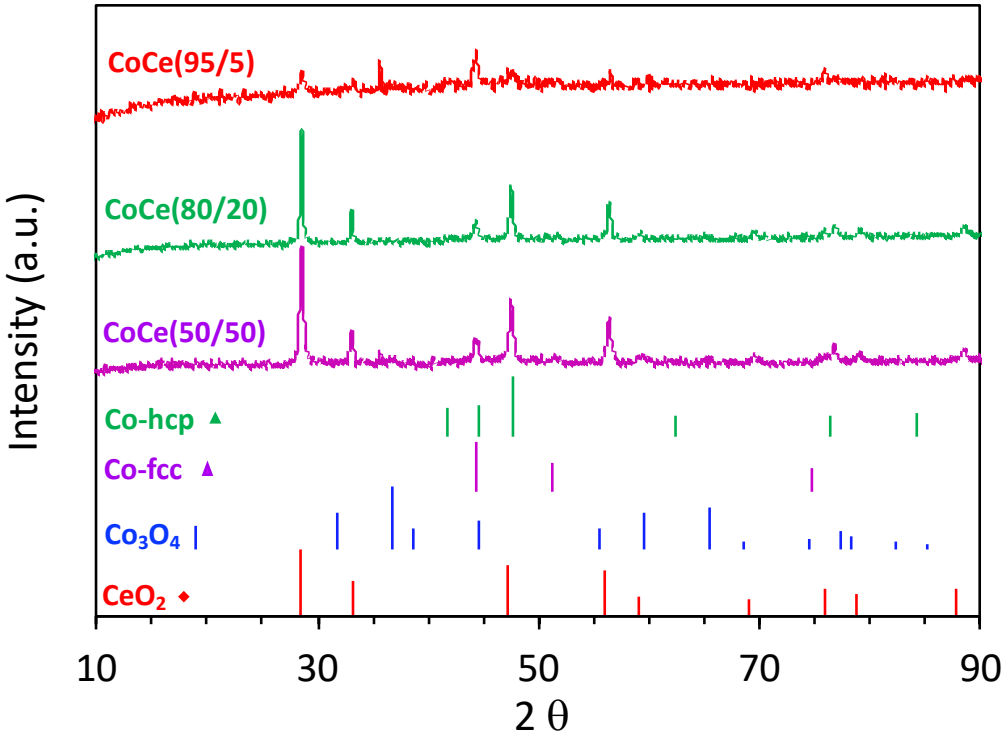

Figure S3. XRD patterns of CoCe catalysts after the catalytic activity measurements under ammonia decomposition reaction conditions (P=1 atm; T=250-550°C; NH_3 flow rate 30 Nml min^{-1}; W_{cat} = 200 mg; WHSV: 9000 mL g^{-1} h^{-1})

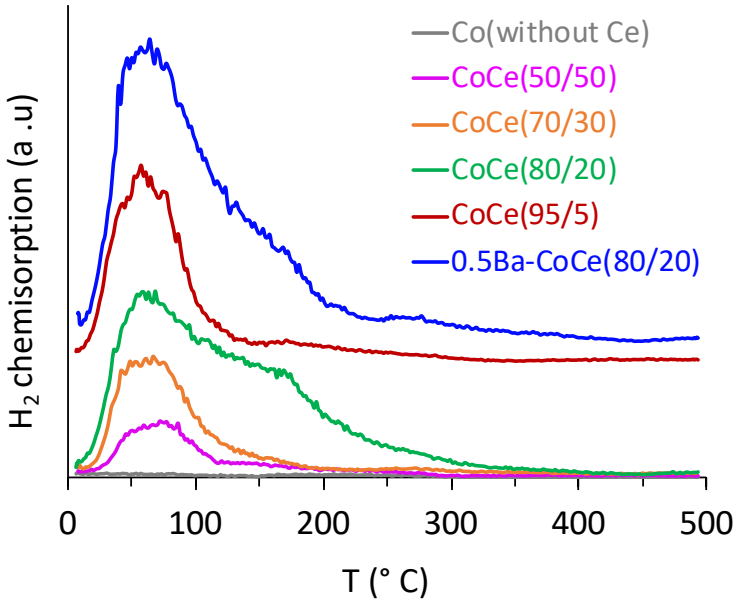

Figure S4. H_2 -TPD curves for catalysts with different CoCe molar ratios and promoted with Ba.

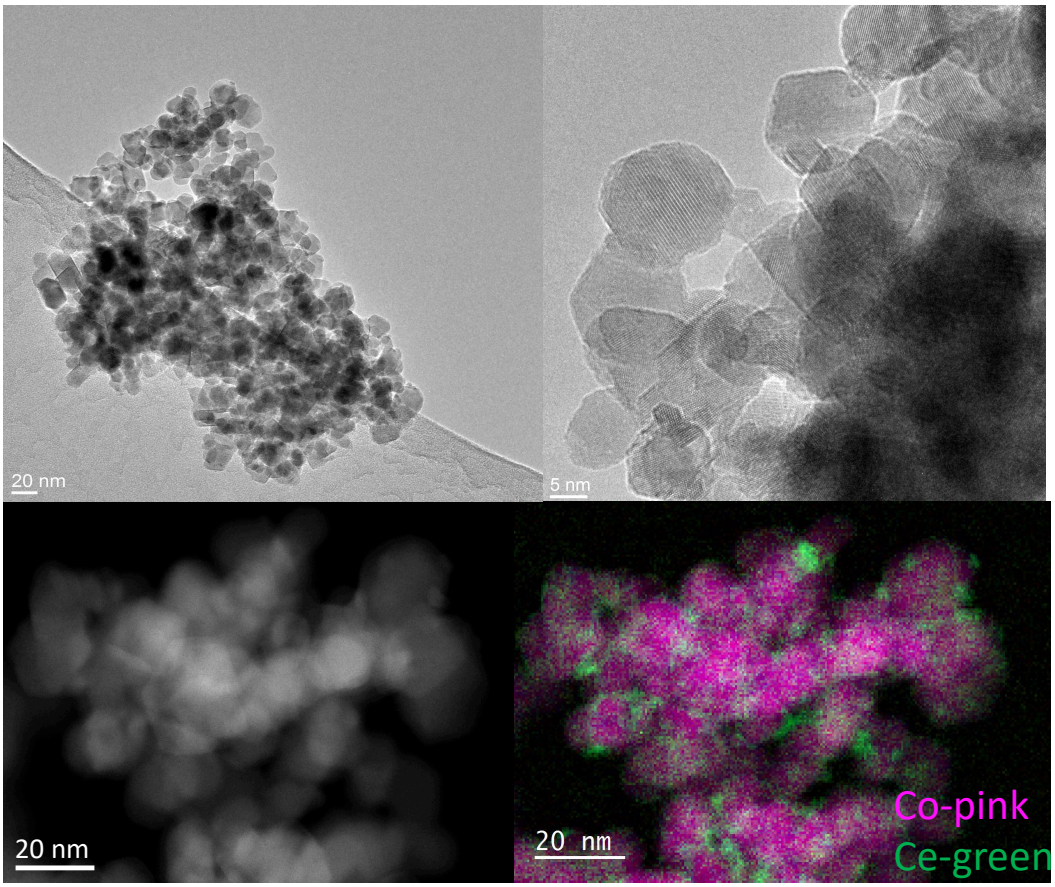

Figure S5. Representative images for CoCe (90/10) after activation under hydrogen 500 °C for 3h, High-Angle Annular Dark-Field Scanning Transmission Electron Microscopy (HAADF– STEM) and Energy-Dispersive X-ray Spectroscopy (EDX). Elemental mapping images for Co(pink), Ce (green).

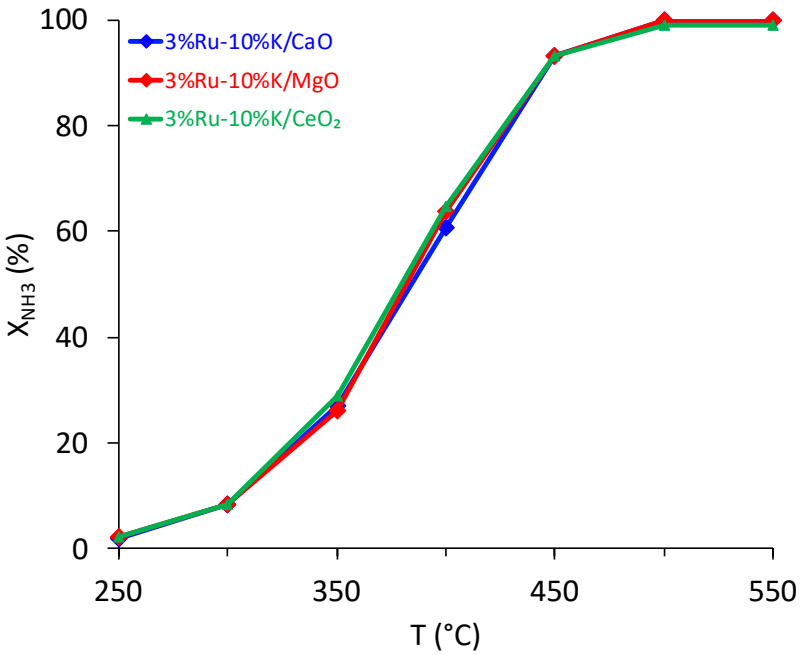

Figure S6. Catalytic performance of Ru catalysts in different supports, CeO_2, CaO, MgO, with 3 %wt. Ru loading and promoted with K (10 % wt.), in ammonia decomposition reaction. Conversion profiles versus reaction temperature. Reaction conditions: P=1 atm; T=250-550°C; NH_3 flow rate 30 Nml min^{-1}; W_{cat} = 200 mg; WHSV: 9000 mL g^{-1} h^{-1}.

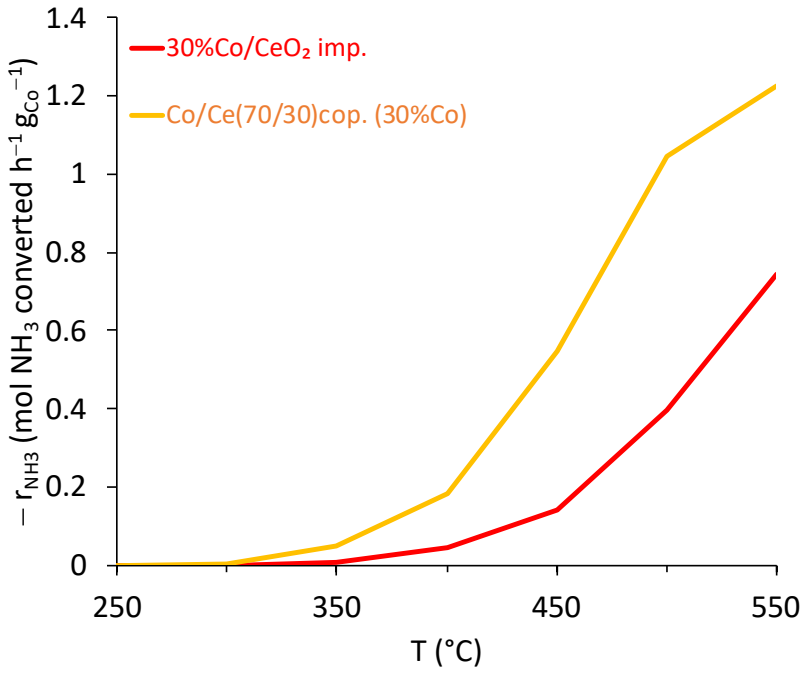

Figure S7. Ammonia conversion reaction rates expressed per gram of Cobalt, of CoCe catalysts with 30 % wt. Co loading, in order to compare the coprecipitation versus impregnation method. Reaction conditions: P=1 atm; T=250-550°C; NH_3 flow rate 30 Nml min^{-1}; W_{cat} = 200 mg; WHSV: 9000 mL g^{-1} h^{-1}.

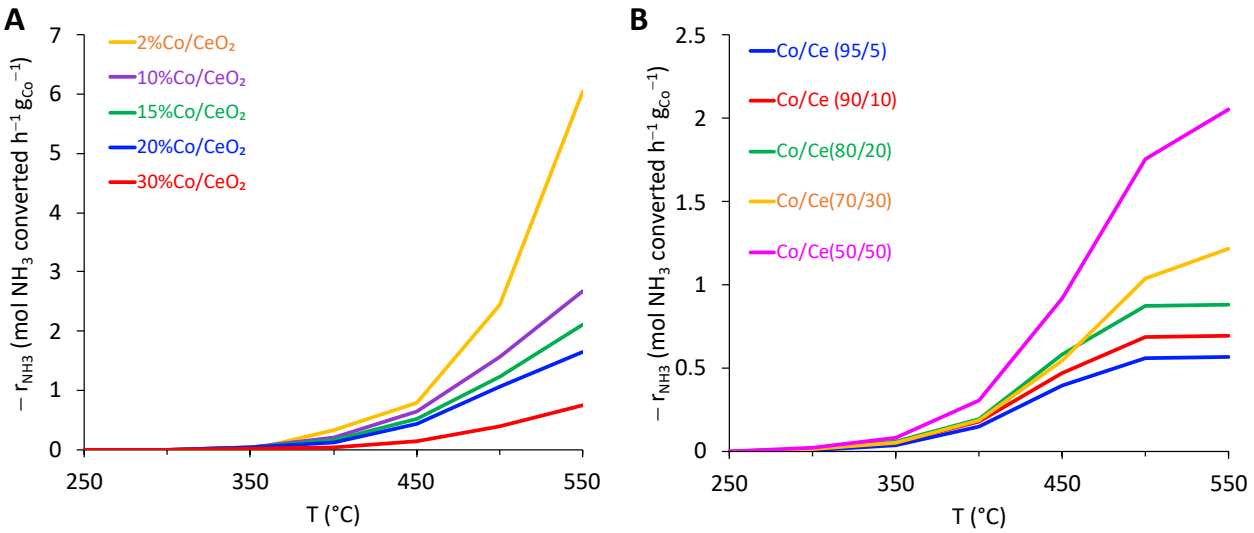

Figure S8. Ammonia conversion reaction rates expressed per gram of Cobalt, of CoCe catalysts prepared by different methods, impregnation coprecipitation, and with several Co loadings. A) Effect of Co loading in samples via impregnation; B) Effect of Co/Ce molar ratio in samples by coprecipitation. Reaction conditions: P=1 atm; T=250-550°C; NH_3 flow rate 30 Nml min^{-1}; W_{cat} = 200 mg; WHSV: 9000 mL g^{-1} h^{-1}.

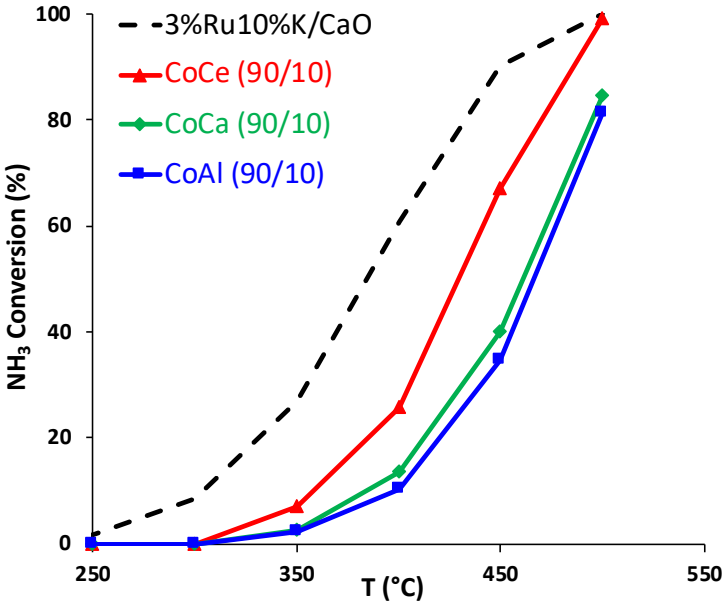

Figure S9. Catalytic performance of Co-catalysts coprecipitated with Al or Ca instead of Ce, in ammonia decomposition reaction. Conversion profiles versus reaction temperature. Reaction conditions: P=1 atm; T=250-550°C; NH_3 flow rate 30 Nml min^{-1}; W_{cat} = 200 mg; WHSV: 9000 mL g^{-1} h^{-1}.

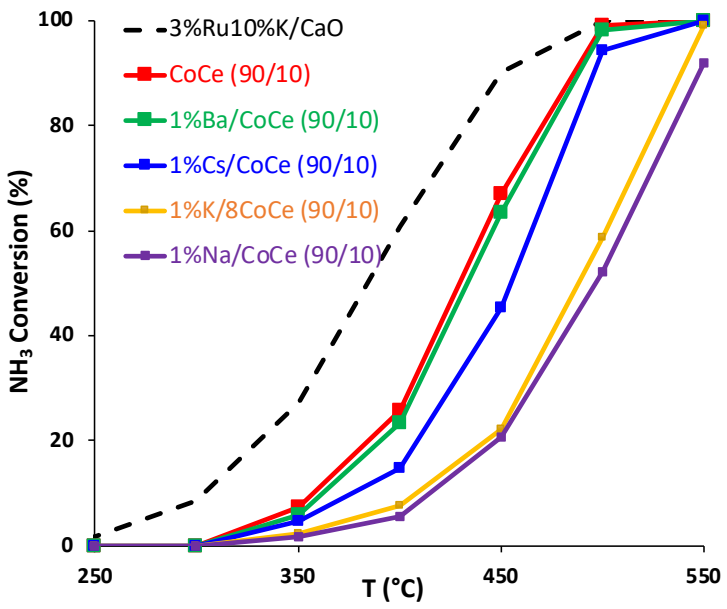

Figure S10. Catalytic performance of CoCe catalysts impregnated with 1% K, Na or Li, in ammonia decomposition reaction. Conversion profiles versus reaction temperature. Reaction conditions: P=1 atm; T=250-550°C; NH_3 flow rate 30 Nml min^{-1}; W_{cat} = 200 mg; WHSV: 9000 mL g^{-1} h^{-1}.

Table S1. Catalytic performance of reported Co-based catalysts for ammonia decomposition reaction. Ammonia conversion and reaction rates are compared.

Catalyst	GHSV (h^{-1})	X_{NH3} (%)		r_{NH3} (mol NH_3 g^{-1} h^{-1})		Reference (year)
		at 450 °C	at 500 °C	at 450 °C	at 500 °C	
0.5% Ba-CoCe (80/20)	**9000**	**80**	**99.9**	**0.294**	**0.368**	**This work**
0.5% Ba-CoCe (80/20)	**22500**	**39**	**61**	**0.363**	**0.561**	**This work**
Co in 1D titanate nanotubes	6000	7	20	0.017	0.049	[14](2019)
Cobalt NP[a] carbon matrix (ZIF 67)	6000	22	55	0.054	0.142	[15](2018)
Cobalt NP in carbon matrix	15000	22	55	0.135	0.337	[16](2017)
Cs-Co_3Mo_3N	6000	50	93	0.123	0.228	[17](2017)
nanocrystalline Co (Al, Ca, K)	19544	41.7	84	0.316	0.552	[18](2016)
Co/MgO-La_2O_3	6000	30	60	0.074	0.147	[19](2016)
Co incorporated in silicalite	15000	-	5	-	0.305	[20-21](2016)
Co/(MgAl-MgCe-MgLa)	6000	28	50	0.069	0.123	[22](2015)
Co NP in alumina matrix	18000	38	72	0.280	0.530	[23](2015)
Co/MWCNTs[b]	6000	-	72	-	0.177	[24](2013)
Core shell Co@SiO_2	30000	5	17	0.061	0.208	[25](2010)
Co-containing CNTs	5000	-	8	-	0.016	[26](2007)

[a]NP: Nanoparticles; [b]MCWCNTs: multiwall carbon nanotubes

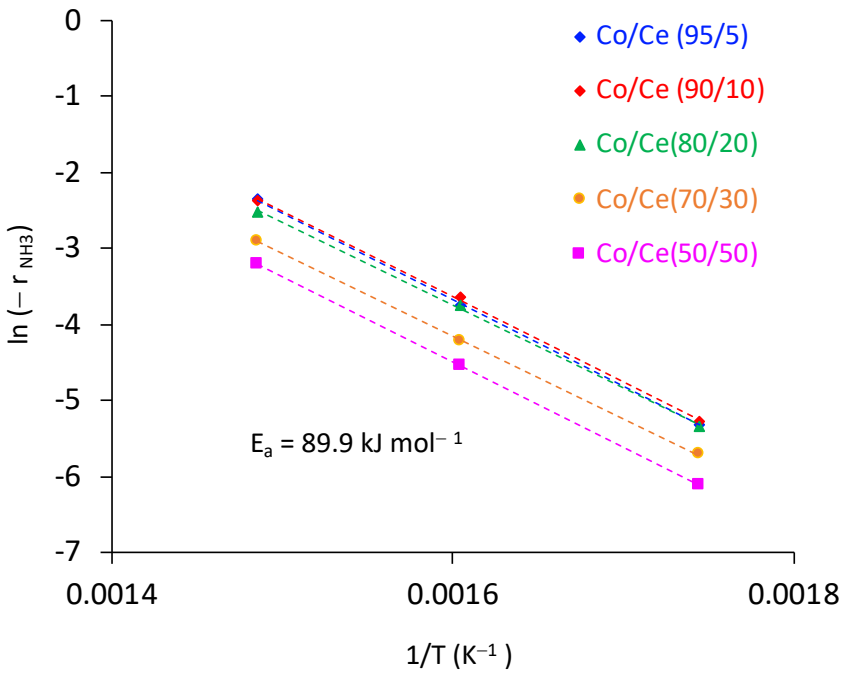

Figure S11. Arrhenius plots in the temperature range 250-400 °C for CoCe catalysts with different CoCe molar ratios. Reaction conditions: P_{atm}, NH_3 flow rate 30 ml/min and WHSV: 9000 mL g^{-1} h^{-1}

References

1. Ju, X.; Liu, L.; Yu, P.; Guo, J.; Zhang, X.; He, T.; Wu, G.; Chen, P., Mesoporous Ru/MgO prepared by a deposition-precipitation method as highly active catalyst for producing COx-free hydrogen from ammonia decomposition. *Applied Catalysis B: Environmental* **2017,** *211*, 167-175.
2. Ju, X.; Liu, L.; Zhang, X.; Feng, J.; He, T.; Chen, P., Highly Efficient Ru/MgO Catalyst with Surface-Enriched Basic Sites for Production of Hydrogen from Ammonia Decomposition. *ChemCatChem* **2019,** *11* (16), 4161-4170.
3. Karim, A. M.; Prasad, V.; Mpourmpakis, G.; Lonergan, W. W.; Frenkel, A. I.; Chen, J. G.; Vlachos, D. G., Correlating Particle Size and Shape of Supported Ru/γ-Al2O3 Catalysts with NH3 Decomposition Activity. *Journal of the American Chemical Society* **2009,** *131* (34), 12230-12239.
4. Karolewska, M.; Truszkiewicz, E.; Mierzwa, B.; Kępiński, L.; Raróg-Pilecka, W., Ammonia synthesis over cobalt catalysts doped with cerium and barium. Effect of the ceria loading. *Applied Catalysis A: General* **2012,** *445-446*, 280-286.
5. Raróg-Pilecka, W.; Karolewska, M.; Truszkiewicz, E.; Iwanek, E.; Mierzwa, B., Cobalt Catalyst Doped with Cerium and Barium Obtained by Co-Precipitation Method for Ammonia Synthesis Process. *Catalysis Letters* **2011,** *141* (5), 678-684.
6. Tarka, A.; Zybert, M.; Kindler, Z.; Szmurło, J.; Mierzwa, B.; Raróg-Pilecka, W., Effect of precipitating agent on the properties of cobalt catalysts promoted with cerium and barium for NH3 synthesis obtained by co-precipitation. *Applied Catalysis A: General* **2017,** *532*, 19-25.
7. Zybert, M.; Tarka, A.; Mierzwa, B.; Kępiński, L.; Raróg-Pilecka, W., Promotion effect of lanthanum on the Co/La/Ba ammonia synthesis catalysts—the influence of lanthanum content. *Applied Catalysis A: General* **2016,** *515*, 16-24.
8. Fu, L.; Bartholomew, C. H., Structure sensitivity and its effects on product distribution in CO hydrogenation on cobalt/alumina. *Journal of Catalysis* **1985,** *92* (2), 376-387.
9. Bergeret, G.; Gallezot, P., Particle Size and Dispersion Measurements. *Handbook of Heterogeneous Catalysis* **2008**, 738-765.
10. Borodziński, A.; Bonarowska, M., Relation between Crystallite Size and Dispersion on Supported Metal Catalysts. *Langmuir* **1997,** *13* (21), 5613-5620.

11. Parastaev, A.; Muravev, V.; Huertas Osta, E.; van Hoof, A. J. F.; Kimpel, T. F.; Kosinov, N.; Hensen, E. J. M., Boosting CO2 hydrogenation via size-dependent metal–support interactions in cobalt/ceria-based catalysts. *Nature Catalysis* **2020,** *3* (6), 526-533.
12. Biesinger, M. C.; Payne, B. P.; Grosvenor, A. P.; Lau, L. W. M.; Gerson, A. R.; Smart, R. S. C., Resolving surface chemical states in XPS analysis of first row transition metals, oxides and hydroxides: Cr, Mn, Fe, Co and Ni. *Applied Surface Science* **2011,** *257* (7), 2717-2730.
13. Pereira-Hernández, X. I.; DeLaRiva, A.; Muravev, V.; Kunwar, D.; Xiong, H.; Sudduth, B.; Engelhard, M.; Kovarik, L.; Hensen, E. J. M.; Wang, Y.; Datye, A. K., Tuning Pt-CeO2 interactions by high-temperature vapor-phase synthesis for improved reducibility of lattice oxygen. *Nature Communications* **2019,** *10* (1), 1358.
14. Lara-García, H. A.; Mendoza-Nieto, J. A.; Pfeiffer, H.; Torrente-Murciano, L., COx-free hydrogen production from ammonia on novel cobalt catalysts supported on 1D titanate nanotubes. *International Journal of Hydrogen Energy* **2019,** *44* (57), 30062-30074.
15. Li, L.; Sun, L.; Cang, H.; Chu, W.; Shao, J.; Yan, J., Silica-assisted mesoporous Co@Carbon nanoplates derived from ZIF-67 crystals and their enhanced catalytic activity. *Journal of Solid State Chemistry* **2018,** *267*, 134-139.
16. Li, L.; Jiang, R.; Chu, W.; Cang, H.; Chen, H.; Yan, J., Cobalt nanoparticles embedded in a porous carbon matrix as an efficient catalyst for ammonia decomposition. *Catalysis Science & Technology* **2017,** *7* (6), 1363-1371.
17. Srifa, A.; Okura, K.; Okanishi, T.; Muroyama, H.; Matsui, T.; Eguchi, K., Hydrogen production by ammonia decomposition over Cs-modified Co3Mo3N catalysts. *Applied Catalysis B: Environmental* **2017,** *218*, 1-8.
18. Czekajło, Ł.; Lendzion-Bieluń, Z., Effect of preparation conditions and promoters on the structure and activity of the ammonia decomposition reaction catalyst based on nanocrystalline cobalt. *Chemical Engineering Journal* **2016,** *289*, 254-260.
19. Podila, S.; Driss, H.; Zaman, S. F.; Alhamed, Y. A.; AlZahrani, A. A.; Daous, M. A.; Petrov, L. A., Hydrogen generation by ammonia decomposition using Co/MgO–La2O3 catalyst: Influence of support calcination atmosphere. *Journal of Molecular Catalysis A: Chemical* **2016,** *414*, 130-139.
20. Varisli, D.; Kaykac, N. G., COx free hydrogen production over cobalt incorporated silicate structured mesoporous catalysts. *Applied Catalysis B: Environmental* **2012,** *127*, 389-398.
21. Varisli, D.; Kaykac, N. G., Hydrogen from ammonia over cobalt incorporated silicate structured catalysts prepared using different cobalt salts. *International Journal of Hydrogen Energy* **2016,** *41* (14), 5955-5968.
22. Podila, S.; Alhamed, Y. A.; AlZahrani, A. A.; Petrov, L. A., Hydrogen production by ammonia decomposition using Co catalyst supported on Mg mixed oxide systems. *International Journal of Hydrogen Energy* **2015,** *40* (45), 15411-15422.
23. Gu, Y.-Q.; Jin, Z.; Zhang, H.; Xu, R.-J.; Zheng, M.-J.; Guo, Y.-M.; Song, Q.-S.; Jia, C.-J., Transition metal nanoparticles dispersed in an alumina matrix as active and stable catalysts for COx-free hydrogen production from ammonia. *Journal of Materials Chemistry A* **2015,** *3* (33), 17172-17180.
24. Zhang, H.; Alhamed, Y. A.; Chu, W.; Ye, Z.; AlZahrani, A.; Petrov, L., Controlling Co-support interaction in Co/MWCNTs catalysts and catalytic performance for hydrogen production via NH3 decomposition. *Applied Catalysis A: General* **2013,** *464-465*, 156-164.
25. Yao, L. H.; Li, Y. X.; Zhao, J.; Ji, W. J.; Au, C. T., Core–shell structured nanoparticles (M@SiO2, Al2O3, MgO; M=Fe, Co, Ni, Ru) and their application in COx-free H2 production via NH3 decomposition. *Catalysis Today* **2010,** *158* (3), 401-408.
26. Zhang, J.; Comotti, M.; Schüth, F.; Schlögl, R.; Su, D. S., Commercial Fe- or Co-containing carbon nanotubes as catalysts for NH3 decomposition. *Chemical Communications* **2007,** (19), 1916-1918.